

A streptavidin variant with slower biotin dissociation and increased mechanostability

Claire E Chivers¹, Estelle Crozat¹, Calvin Chu², Vincent T Moy², David J Sherratt¹ & Mark Howarth¹

Streptavidin binds biotin conjugates with exceptional stability but dissociation does occur, limiting its use in imaging, DNA amplification and nanotechnology. We identified a mutant streptavidin, traptavidin, with more than tenfold slower biotin dissociation, increased mechanical strength and improved thermostability; this resilience should enable diverse applications. FtsK, a motor protein important in chromosome segregation, rapidly displaced streptavidin from biotinylated DNA, whereas traptavidin resisted displacement, indicating the force generated by Ftsk translocation.

The remarkably strong interaction between the small molecule biotin and the proteins streptavidin or (neutr)avidin is widely exploited in biological research¹. Biotin-binding proteins have been isolated from a wide range of species, but streptavidin binds the most stably to biotin conjugates¹. Streptavidin is used in imaging, protein purification and nano-assembly, and is showing success in cancer clinical trials. Streptavidin and biotin have low nonspecific binding and biotinylation generally does not disrupt biomolecule function. Alternative targeting methods, such as those using HaloTag or SNAP-tag, form irreversible covalent bonds to their ligand and are valuable for cellular labeling². However, these domains do not have the resistance of streptavidin to temperature, pH or denaturant, and so even though prebound ligand will remain attached under these harsh conditions, these covalent-binding proteins may unfold, aggregate and promote nonspecific binding. Also, unlike SNAP-tag and HaloTag ligands, biotin can be precisely targeted to proteins *in vitro*, on cells and in living animals using biotin ligase¹. An additional advantage is that many streptavidin and biotin conjugates are commercially available.

Despite its stable binding, the perception that the streptavidin-biotin interaction is essentially irreversible is far from correct. For example, in imaging, low endosomal pH led to dissociation of streptavidin being detected in 2 h, whereas the receptor of interest had a lifetime of ~4 days³. Also, nanoparticle attachment can cause a surprising decrease in streptavidin-biotin stability⁴; the

dissociation constant (K_d) for a biotinylated peptide increased approximately a million-fold when streptavidin was attached to beads⁵. In the presence of shear forces lower than those in a blood capillary, streptavidin-coated beads do not attach to a biotinylated surface but instead roll across, with arrests of 20 ms to tens of seconds⁶. In addition, streptavidin cannot prevent the translocation of molecular motors such as helicases, RNA polymerase or DNA polymerase along DNA⁷. Streptavidin can be used at high temperatures, such as for PCR, BEAMing and 454 DNA sequencing, but DNA has to be bis-biotinylated to reduce dissociation⁸.

A streptavidin mutant containing a cysteine forms a disulfide with a thiol-linked biotin conjugate, giving controlled reversibility⁹, but this mutant only enhances binding to certain biotin conjugates and in systems unaffected by changing redox state, precluding use in cells. We therefore aimed to engineer a streptavidin mutant that would bind more stably to any biotin conjugate.

In a highly optimized system, almost any change reduces performance. Over 200 streptavidin mutants have been described but none have improved biotin-binding stability¹. Streptavidin libraries have been screened for various properties by phage display and *in vitro* compartmentalization, yielding, for example, a streptavidin variant with improved desthiobiotin binding, but no pair with as strong binding as wild-type streptavidin-biotin has been identified^{10,11}. Based on this literature, we avoided mutations near the ureido or thiophene rings of biotin, which invariably impair binding¹, and explored many mutations adjacent to the biotin carboxyl and in the L3/4 loop^{1,10,11}. We randomized promising residues and evaluated purified proteins according to biotin-4-fluorescein dissociation ('off') rate and found the lowest off rate for the S52G,R53D mutant of streptavidin (**Fig. 1a**), which we termed traptavidin. We hypothesize that the mutations in traptavidin reduce flexibility of the L3/4 loop (residues 45–50; **Fig. 1a**). Upon biotin binding, this loop becomes ordered and closes over the biotin-binding pocket¹². A more ordered loop may reduce the entropic cost of biotin binding and inhibit dissociation as well as decrease the association ('on') rate and enhance thermostability.

The off rate for free biotin at 37 °C and pH 7.4 was more than tenfold lower for traptavidin than streptavidin ($4.2 \pm 0.5 \times 10^{-6} \text{ s}^{-1}$ for traptavidin and $6.8 \pm 0.3 \times 10^{-5} \text{ s}^{-1}$ for streptavidin; **Fig. 1b**). As a substantial part of (strept)avidin's binding energy comes from interaction with the carboxyl group of biotin¹, it is important to establish how derivatization at the carboxyl group changes binding strength. Traptavidin also had a dramatically reduced off rate to biotin conjugates ($P = 0.0008$; **Fig. 1c**). After the ~2% dissociation at the initial time point, there was little dissociation from traptavidin over the subsequent 12 h. In contrast, streptavidin dissociated steadily, and avidin dissociated even faster than streptavidin¹. At pH 5, traptavidin dissociation was faster than at pH 7.4 but was still significantly slower than streptavidin dissociation ($P = 0.001$) (**Fig. 1d**). The on rate of

¹Department of Biochemistry, Oxford University, Oxford, UK. ²Department of Physiology and Biophysics, University of Miami, Miller School of Medicine, Miami, Florida, USA. Correspondence should be addressed to M.H. (mark.howarth@bioch.ox.ac.uk).

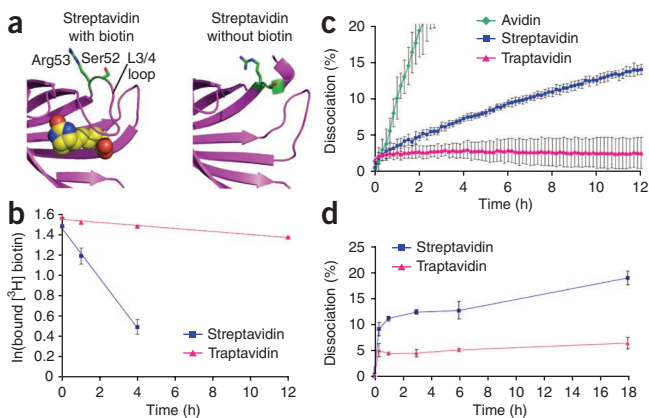


Figure 1 | Traptavidin has a slower dissociation rate from biotin conjugates compared to streptavidin. **(a)** PyMOL images showing the residues mutated to produce traptavidin (S52G,R53D) in structures of streptavidin with biotin (1mk5) and without biotin (1swa). Biotin is shown as spheres of van der Waals radius. Ser52 and Arg53 are colored green. Without biotin, the L3/4 loop is disordered and does not give clear electron density. **(b)** Streptavidin and traptavidin off rates, measured by binding the proteins to [³H]biotin, then adding excess nonradioactive biotin and determining the fraction of [³H]biotin remaining bound after varying times at 37 °C and pH 7.4. **(c)** Dissociation rates of traptavidin, streptavidin and avidin at pH 7.4. The proteins bind to biotin-4-fluorescein, quenching its fluorescence; upon addition of excess free biotin, biotin-4-fluorescein dissociates, and the increase in fluorescence was measured at 37 °C. **(d)** Traptavidin and streptavidin dissociation rates at pH 5.0, analyzed as in **c**. Error bars, 1 s.d. ($n = 3$). Some error bars are too small to be visible.

traptavidin for biotin-4-fluorescein was reduced twofold, from $2.0 \pm 0.1 \times 10^7 \text{ M}^{-1} \text{ s}^{-1}$ for streptavidin to $1.0 \pm 0.03 \times 10^7 \text{ M}^{-1} \text{ s}^{-1}$ for traptavidin ($P = 0.004$), whereas the on rate of traptavidin for [³H]biotin was also reduced (**Supplementary Fig. 1**). The slower on rate of traptavidin means that longer incubations are required to reach equilibrium.

Streptavidin is often used at high temperature. Traptavidin had increased thermostability compared to streptavidin before splitting into monomers; the midpoint of transition was ~ 10 °C higher than for streptavidin (**Fig. 2a**). We also assessed biotin-conjugate binding stability at high temperatures (**Fig. 2b**). At 70 °C, there was complete dissociation from streptavidin, but most ligand was still bound to traptavidin.

Imaging of cell-surface proteins using biotin ligase and streptavidin is rapid and sensitive, and the target protein needs only to be modified with a 15-amino-acid tag. The altered

charge of traptavidin may affect nonspecific cellular binding, as seen for avidin compared to lower-pI mutants¹. We investigated whether traptavidin had similar specificity to streptavidin in mammalian cells. We fused the type 1 insulin-like growth factor receptor IGF1R to the acceptor peptide (AP-IGF1R), biotinylated the acceptor peptide with co-expressed biotin ligase (BirA-ER) and detected biotinylated AP-IGF1R with fluorescently labeled traptavidin or streptavidin (**Supplementary Fig. 2**). Traptavidin showed high specificity for imaging, with a strong signal on cells expressing AP-IGF1R and BirA-ER, and minimal binding when we pre-blocked traptavidin with biotin. Staining with traptavidin and streptavidin was comparable (**Supplementary Fig. 2**). However, with shorter staining durations, the cell staining was more intense with streptavidin (data not shown), consistent with the slower on rate of traptavidin.

The relationship between binding stability over time versus resistance to force is complex: force changes the height and landscape of the activation energy for dissociation. We probed the mechanical strength of traptavidin at the single-molecule level by atomic force microscopy (AFM). Traptavidin had greater mechanical binding stability than streptavidin over a range of loading rates ($P < 0.0001$) (**Fig. 3a**). We observed a distribution of binding strengths (**Supplementary Fig. 3a**) because of the importance of thermal fluctuations to traversing the activation barrier. From the relationship between loading rate and rupture force, we could estimate the difference in the dissociation rate between streptavidin and traptavidin at a given force (**Supplementary Fig. 3b**).

We applied traptavidin to study FtsK, one of the fastest molecular motor proteins, translocating along DNA at 5 kb s^{-1} (refs. 13,14). Before bacteria divide, FtsK translocates along DNA until encountering XerC and XerD; then FtsK activates site-specific recombination by XerC/D, separating chromosome dimers and ensuring faithful partition of one chromosome to each daughter cell. *In vivo* DNA is bound to many proteins, including repressors, transcription factors, RNA polymerases and DNA-bending architectural proteins. To study how *Pseudomonas aeruginosa* FtsK copes with obstacles in its path, we used a short DNA substrate containing KOPS, an 8-bp sequence that loads FtsK directionally^{13,14}, with a biotinylated nucleotide near the end, so that FtsK would load on to the DNA in a defined orientation and then translocate until encountering streptavidin or traptavidin bound to the biotin (**Fig. 3b**).

Despite the strength of the streptavidin-biotin interaction, $0.5 \mu\text{M}$ FtsK displaced the majority of streptavidin from the DNA within 3 min, whereas traptavidin resisted displacement (**Fig. 3c**).

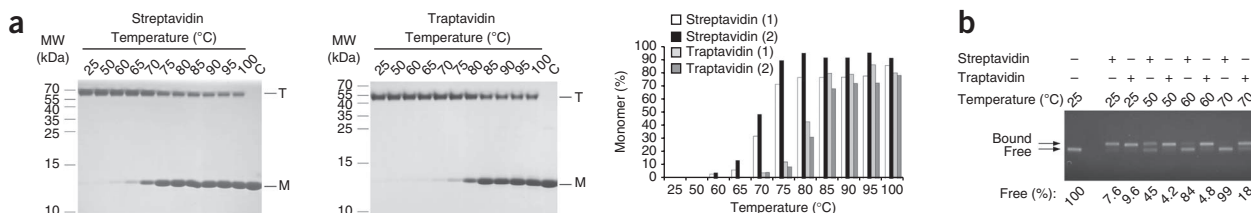


Figure 2 | Traptavidin has increased thermostability compared to streptavidin. **(a)** Thermostability analysis of tetramer structure of streptavidin (left) or traptavidin (middle). Proteins were incubated for 3 min at the indicated temperatures, and then separated by SDS-PAGE and Coomassie stained. The positive control (C) was mixed with SDS before heating at 95 °C. Tetramer (T) and monomer (M) bands are indicated. The percentage of monomers from duplicate gels (indicated as 1 and 2) was plotted (right). **(b)** Thermostability of biotin-conjugate binding. Streptavidin or traptavidin were incubated with biotinylated DNA and heated for 3 min at the indicated temperatures before agarose gel electrophoresis and fluorescence imaging of DNA. The left lane is a negative control with no streptavidin or traptavidin added. Bands corresponding to DNA that is free or bound to streptavidin or traptavidin are marked. The percentage of biotinylated DNA free from streptavidin or traptavidin is labeled under each lane.

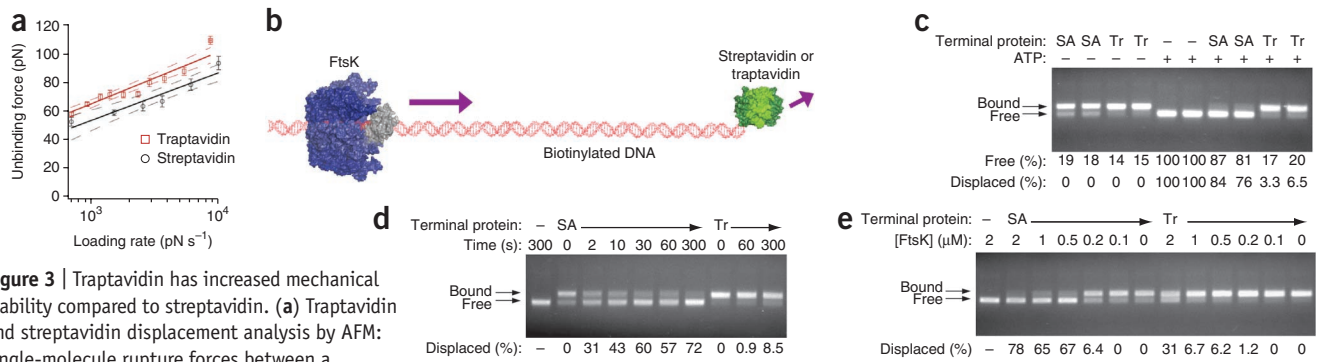


Figure 3 | Traptavidin has increased mechanical stability compared to streptavidin. **(a)** Traptavidin and streptavidin displacement analysis by AFM: single-molecule rupture forces between a biotinylated bead and an AFM tip coated with streptavidin or traptavidin were measured at the indicated loading rates. Means are shown \pm 1 s.e.m. (streptavidin, $n = 400$ and traptavidin, $n = 562$), with best fits and 95% confidence limits indicated by solid and dashed lines, respectively. **(b)** Cartoon of motor assay showing DNA containing a loading site for FtsK and a biotinylated thymidine near the terminus that was capped with traptavidin or streptavidin (green). FtsK α and β domains are shown in blue and γ in gray. In the presence of ATP, FtsK translocates along the DNA and collides with streptavidin or traptavidin. **(c)** Displacement of streptavidin (SA) or traptavidin (Tr) by FtsK after 180 s was determined by gel electrophoresis, with DNA fluorescence visualized. FtsK does not remain bound to DNA upon electrophoresis, but bound streptavidin or traptavidin causes the gel shift indicated with arrows. Controls are shown without streptavidin or traptavidin or without ATP, preventing FtsK activity. The percentage of free DNA and the percentage of DNA displaced by FtsK for duplicate assays are indicated under each lane. **(d)** Streptavidin or traptavidin displacement by FtsK analyzed by incubating each protein with FtsK for the indicated times (analyzed as in **c**). **(e)** Traptavidin is displaced by a high concentration of FtsK. Streptavidin and traptavidin displacement by varying amounts of FtsK analyzed by incubating each protein for 180 s with the indicated concentration of FtsK (analyzed as in **c**).

Streptavidin displacement was detectable after only 2 s, but we observed little displacement of traptavidin even after 300 s (**Fig. 3d**). Increasing the FtsK concentration to 2 μ M allowed substantial displacement of traptavidin (**Fig. 3e**), indicating that multiple FtsK motors could cooperate in exerting a stronger force. Traptavidin was equally as strong a roadblock to *Escherichia coli* FtsK and with DNA biotinylated at the 5' terminus rather than at an internal thymidine (**Supplementary Fig. 4**). As FtsK rapidly broke the stable biotin-streptavidin interaction, *in vivo* FtsK should be sufficient to displace even strongly attached DNA-binding proteins.

The stall force for FtsK measured by pulling on the DNA with optical tweezers is > 65 pN, at which point the DNA double helix itself is deformed¹⁴. Traptavidin displacement should enable testing of higher forces without distorting the DNA. Streptavidin has previously been used as an obstacle to motors⁷, providing a simpler method to probe force generation than single-molecule assays^{13,14}. However, only wild-type streptavidin and the weak nitroavidin have been used⁷, so traptavidin and the range of weaker streptavidin mutants¹ could be used to generate a calibration curve to dissect force generation by proteins¹⁵.

Traptavidin binding was more stable for a range of biotin conjugates (**Supplementary Fig. 5**), not just one particular ligand. Also, traptavidin can be recombinantly expressed in comparable yields to streptavidin, and recombinant expression of streptavidin gives yields higher than purification from *Streptomyces avidinii*¹⁶. Therefore, traptavidin has the potential to replace streptavidin in many applications in which dissociation is a limitation, for example, when used as a molecular anchor for arrays, surface-plasmon resonance or point-of-care diagnostics. Traptavidin-biotin recognition may also aid our understanding of the subtle intermolecular forces that govern interactions of extreme stability.

METHODS

Methods and any associated references are available in the online version of the paper at <http://www.nature.com/naturemethods/>.

Accession codes. GenBank: GU952124.

Note: Supplementary information is available on the Nature Methods website.

ACKNOWLEDGMENTS

Funding was provided by the Wellcome Trust (M.H., D.J.S. and E.C.), the Biotechnology and Biological Sciences Research Council (C.E.C.), the US National Institutes of Health (V.T.M. and C.C.), the National Science Foundation (V.T.M.), the University of Miami (V.T.M.) and Worcester College Oxford (M.H.). We thank J.E. Graham and I. Grainge for helpful discussion.

AUTHOR CONTRIBUTIONS

C.E.C., M.H., E.C., V.T.M. and C.C. performed the research; M.H., V.T.M. and D.J.S. designed research; all analyzed the data; M.H., D.J.S. and C.E.C. wrote the manuscript.

COMPETING FINANCIAL INTERESTS

The authors declare competing financial interests: details accompany the full-text HTML version of the paper at <http://www.nature.com/naturemethods/>.

Published online at <http://www.nature.com/naturemethods/>.

Reprints and permissions information is available online at <http://npg.nature.com/reprintsandpermissions/>.

- Laitinen, O.H., Hytonen, V.P., Nordlund, H.R. & Kulomaa, M.S. *Cell. Mol. Life Sci.* **63**, 2992–3017 (2006).
- Sletten, E.M. & Bertozzi, C.R. *Angew. Chem. Int. Edn. Engl.* **48**, 6974–6998 (2009).
- Bruneau, E., Sutter, D., Hume, R.I. & Akaaboune, M. *J. Neurosci.* **25**, 9949–9959 (2005).
- Swift, J.L., Heuff, R. & Cramb, D.T. *Biophys. J.* **90**, 1396–1410 (2006).
- Buranda, T., Lopez, G.P., Keij, J., Harris, R. & Sklar, L.A. *Cytometry* **37**, 21–31 (1999).
- Pierres, A., Touchard, D., Benoliel, A.M. & Bongrand, P. *Biophys. J.* **82**, 3214–3223 (2002).
- Morris, P.D., Tackett, A.J. & Raney, K.D. *Methods* **23**, 149–159 (2001).
- Dressman, D., Yan, H., Traverso, G., Kinzler, K.W. & Vogelstein, B. *Proc. Natl. Acad. Sci. USA* **100**, 8817–8822 (2003).
- Wu, S.C., Ng, K.K. & Wong, S.L. *Proteins* **77**, 404–412 (2009).
- Aslan, F.M., Yu, Y., Mohr, S.C. & Cantor, C.R. *Proc. Natl. Acad. Sci. USA* **102**, 8507–8512 (2005).
- Levy, M. & Ellington, A.D. *Chem. Biol.* **15**, 979–989 (2008).
- Freitag, S., Le Trong, I., Klumb, L., Stayton, P.S. & Stenkamp, R.E. *Protein Sci.* **6**, 1157–1166 (1997).
- Graham, J.E., Sivanathan, V., Sherratt, D.J. & Arciszewska, L.K. *Nucleic Acids Res.* **38**, 72–81 (2010).
- Pease, P.J. *et al. Science* **307**, 586–590 (2005).
- Crozat, E. *et al. EMBO J.* **29**, 1423–1433 (2010).
- Gallizia, A. *et al. Protein Expr. Purif.* **14**, 192–196 (1998).

ONLINE METHODS

General. Biotin (Sigma) was dissolved in DMSO at 100 mM. Avidin (Sigma) was dissolved in PBS at 23 μM . SDS-PAGE was performed at 200 V with the gel box (X Cell SureLock; Invitrogen) surrounded by ice to prevent dissociation of the streptavidin subunits during electrophoresis. Structures of streptavidin without biotin (1swa) and with biotin (1mk5) were displayed and aligned using PyMOL (DeLano Scientific). The cartoon in **Figure 3b** was constructed with PyMOL based on crystal structures 1swe, 2iuu and 2ve9. Note that FtsK- γ is shown in the conformation bound to KOPS and is likely to change when translocating¹³.

Plasmid construction. Streptavidin in this paper refers to core streptavidin with 6His at the C terminus, with the gene encoding the protein in pET21a(+). Traptavidin was generated by introducing the S52G,R53D mutation into streptavidin by QuikChange (Stratagene) mutagenesis using the primer S52G R53D F (**Supplementary Table 1**) and its reverse complement. The mutations were confirmed by DNA sequencing. AP-IGF1R was constructed from pcDNA3 containing human IGF1R (a kind gift from V. Macaulay, University of Oxford) by PCR-amplifying two fragments: the first fragment with primers IGFA and IGFB and the second fragment with primers IGFC and IGFD (**Supplementary Table 1**). The fragments were joined by overlap extension PCR, digested with NheI and NotI and ligated into pcDNA3.1. The acceptor peptide¹⁷ (GLNDIFEAQKIEWHE) was thus inserted after the IGF1R signal sequence along with a 6-amino-acid spacer sequence before the start of sequence encoding the N terminus of mature IGF1R. BirA-ER (*E. coli* biotin ligase targeted to the endoplasmic reticulum) and pECFP-H2B (human histone H2B fused to enhanced CFP) have been previously described¹⁸.

Streptavidin and traptavidin expression and purification. An overnight culture of streptavidin or traptavidin, picked from a freshly grown colony of *E. coli* BL21 (DE3) RIPL (Stratagene), was diluted 100-fold into LB ampicillin, grown to OD_{600} 0.9 at 37 °C, induced with 0.5 mM IPTG and incubated for an additional 4 h at 37 °C. Inclusion bodies were isolated from the cell pellet of a 750 ml culture by rocking with 10 ml 300 mM NaCl, 50 mM Tris, 5 mM EDTA, 0.8 mg ml⁻¹ lysozyme, 1% Triton X-100 pH 7.8 for 30 min at 25 °C followed by 9 min of pulsed sonication on ice at 40% amplitude on a Sonics Vibra-Cell sonicator. After centrifugation at 27,000g for 15 min, the inclusion body pellet was washed three times in 10 ml 100 mM NaCl, 50 mM Tris, 0.5% Triton X-100 (pH 7.8) and then dissolved in 6 M guanidinium hydrochloride (pH 1.5) (GuHCl). Protein in GuHCl was refolded by rapid dilution into PBS at 4 °C and stirring overnight¹⁹. Ni-NTA resin (Qiagen), equilibrated in 300 mM NaCl, 50 mM Tris, 10 mM imidazole (pH 7.8), was added and rotated overnight at 4 °C. The next day, the resin was isolated by centrifugation, washed once with 5 ml of 300 mM NaCl, 50 mM Tris, 30 mM imidazole (pH 7.8) and then added to a poly-prep column (Bio-Rad) for elution with 5 ml 300 mM NaCl, 50 mM Tris, 200 mM imidazole (pH 7.8). The eluate was dialyzed three times against PBS. Protein concentration was determined after dialysis from OD_{280} using ϵ_{280} of 34,000 M⁻¹cm⁻¹ (ref. 20). Typical yields were 8 mg per liter of culture for streptavidin and 5 mg per liter of culture for traptavidin. Streptavidin and traptavidin were labeled with Alexa

Fluor 555 by adding 1/10 volume of 1 M NaHCO₃ (pH 8.3) and then a tenfold molar excess of Alexa Fluor 555 succinimidyl ester (Invitrogen) (stock dissolved at 1 mg ml⁻¹ in dry dimethylformamide) and incubating for 4 h at 25 °C. Free dye was separated using 1 ml packed volume Sephadex G-25 (Sigma) in a poly-prep column. Fractions containing labeled protein were pooled and free dye was removed by three rounds of dialysis in PBS.

Biotin–4-fluorescein off-rate assay. The off rate of biotin–4-fluorescein from avidin, streptavidin or traptavidin was measured using a PHERAstar plate-reader with 480 nm excitation and 520 nm emission (BMG LabTech). In this assay, the binding of biotin–4-fluorescein to an excess of binding protein results in quenching of fluorescein emission²¹. As the biotin–4-fluorescein dissociates, the fluorescence recovers. The assay was performed using excess biotin, so that sites left open by biotin–4-fluorescein dissociation are re-filled by biotin immediately. We added 1 μM protein in 10 μl of PBS to 12 nM biotin–4-fluorescein (Invitrogen) with 0.12 mg ml⁻¹ BSA in 170 μl of PBS and incubated the solutions for 1 h at 37 °C. Then, 20 μl PBS or 20 μl 1 mM biotin in PBS was added, and fluorescence measurements were immediately started at 37 °C. Percentage dissociation was calculated as (signal with biotin – signal without biotin)/(signal without quenching – signal without biotin) \times 100. For the signal without quenching, no biotin-binding protein was added to the biotin–4-fluorescein (B4F).

For the low pH off-rate assay, 100 nM streptavidin or traptavidin was incubated with 12 nM B4F in 100 mM NaCl with 30 mM sodium citrate (pH 5.0) for 3 h at 25 °C before incubating at 37 °C with 100 μM biotin for 0.5, 1, 3, 6 and 18 h. As B4F fluorescence is decreased at low pH, samples were then placed on ice to block further dissociation, adjusted to pH 7.2 with 1 M HEPES at pH 8.3, and fluorescence intensity was immediately measured as above. *P* values were calculated using two-tailed Student's *t*-tests from the triplicate data at the 6 h time point.

[³H]biotin off-rate assay. The dissociation kinetics of biotin from streptavidin and traptavidin were determined using a method modified from that described previously²². We incubated 10 nM 8,9-^{[3}H]biotin (PerkinElmer LAS) for 1 h at 25 °C with 250 nM streptavidin or traptavidin in PBS. To initiate dissociation, non-radioactive biotin was added to a final concentration of 50 μM and incubated at 37 °C. At each time point, the protein-biotin complex was pulled down by incubation with a 50% slurry of Ni-NTA resin, equilibrated in 300 mM NaCl, 50 mM Tris, 10 mM imidazole (pH 7.8), for 1 h at 25 °C, followed by centrifugation. Then, 25 μl supernatant, containing unbound radioactive biotin, was added to the scintillation cocktail and counted in a liquid scintillation counter (LS-5000TD; BeckmanCoulter). The average radioactivity of the supernatant at each time point (*x*) and the radioactivity of the protein-biotin complex before addition of cold biotin (*a*) enabled the first-order dissociation rate constant to be determined from the plot of $\ln(\text{fraction bound})$ ($\ln(a - x/a)$) against time. Excel was used for linear regression and to calculate error bars, using the “LINEST” linear least-squares curve-fitting routine.

Biotin–4-fluorescein on-rate assay. The on rate of B4F for streptavidin or traptavidin was measured in PBS on a PHERAstar plate-reader. We added 20 μl of 10 nM streptavidin or traptavidin

to 180 μl of 56 pM B4F and measured the fluorescein emission every 6 s at 25 °C. The on rate was too fast to measure using this approach at 37 °C. The concentration of free B4F was calculated as (signal with B4F – signal without B4F)/(signal without protein – signal without B4F) \times 50 pM starting B4F. Linear regression using GraphPad Prism (GraphPad Software) was applied to the plot of $\ln([\text{free biotin} - 4\text{-fluorescein}])$ against time, with the gradient equal to $k_{\text{on}} \times ([\text{streptavidin or traptavidin}])$. Error bars for the on rate were calculated using the “LINEST” linear least-squares curve-fitting routine in Excel (Microsoft).

[³H]biotin on-rate assay. The on rate of biotin was determined by incubating 250 pM streptavidin or traptavidin with 1 nM [³H]biotin in PBS at 37 °C. Binding was stopped by addition of 50 μM nonradioactive biotin. Protein was pulled down by incubation with 50% slurry of Ni-NTA resin, equilibrated in 300 mM NaCl, 50 mM Tris, 10 mM imidazole (pH 7.8), for 1 h at 25 °C (in this time at 25 °C dissociation of [³H]biotin is negligible²⁰), followed by centrifugation. Then 25 μl of supernatant containing unbound [³H]biotin was added to scintillation cocktail and counted in a liquid scintillation counter (Wallac 1409; PerkinElmer). We measured the radioactivity of the supernatant in cpm at each time point and the total radioactivity present before addition of protein, to calculate free [³H]biotin concentration. The second-order association rate constant was then determined from the plot of $1/([\text{free } ^3\text{H}]\text{biotin})$ against time. Excel was used for linear regression and to calculate error bars, using the “LINEST” linear least-squares curve-fitting routine.

Equilibrium dissociation constant. K_{d} was calculated from $k_{\text{off}}/k_{\text{on}}$. The s.d. of this quotient was calculated with the formula $(A \pm a)/(B \pm b) = (C \pm c)$, where $c = C \times \sqrt{((a/A)^2 + (b/B)^2)}$, in which A , B and C are k_{off} , k_{on} and K_{d} , respectively, with lowercase letters representing the s.d. Our k_{on} and k_{off} for streptavidin are comparable with previous values^{23,24}. The literature K_{d} value for streptavidin-biotin²⁵ (4×10^{-14} M) was determined at 25 °C, but it is known that the off rate of streptavidin dramatically increases with temperature^{23,26}.

Thermostability assay. To determine tetramer stability, 3 μM streptavidin or traptavidin in PBS was heated at the indicated temperature for 3 min in a Bio-Rad DNA Engine Peltier Thermal Cycler and then immediately placed on ice^{27–29}. Samples were mixed with 6 \times SDS-PAGE loading buffer and loaded onto an 18% polyacrylamide gel. The 100% monomer positive control was mixed with SDS loading buffer before heating at 95 °C for 3 min. Band intensities were quantified using a ChemiDoc XRS imager and QuantityOne 4.6 software (Bio-Rad). Note that the tetramer band does not run according to molecular weight as its position is influenced by protein charge.

To determine thermostability of biotin conjugate binding, 5.0 μM streptavidin or traptavidin in PBS was incubated with 21 nM monobiotinylated DNA in a volume of 4 μl for 30 min at 25 °C. Samples were made up to 10 μl with a final concentration of 100 μM biotin, 20 mM Tris acetate, 1 mM DTT, 2 mM magnesium acetate and 20 mM potassium glutamate (pH 7.5) and incubated for 5 min at 25 °C, before heating at the indicated temperature for 3 min in a Thermal Cycler and cooling to 10 °C. A 1.5% agarose gel was run at 6.0 V cm^{-1} in TAE for 45 min at 25 °C and ethidium

bromide-stained DNA was visualized on a ChemiDoc XRS imager using QuantityOne 4.6 software. Percentages were defined as 100 \times the intensity of the band for free DNA divided by the summed intensities of the bands for free and bound DNA. The 439-bp monobiotinylated DNA was prepared by PCR using Taq DNA polymerase with the primers Fts1 and the internally biotinylated primer bioFts2 (Eurofins) (**Supplementary Table 1**) from plasmid pJEG41-N1, a derivative of pUC18 containing a lambda phage insert.

Cell culture, biotinylation and imaging. COS7 cells were grown in DMEM with 10% fetal calf serum, 50 U ml^{-1} penicillin and 50 $\mu\text{g ml}^{-1}$ streptomycin. Cells were transfected using Lipofectamine 2000 (Invitrogen) following manufacturer’s instructions with 0.25 μg AP-IGF1R, 0.2 μg BirA-ER and 0.05 μg H2B-ECFP per well of a 48 well plate. Cells were incubated with 10 μM biotin overnight for optimum biotinylation by BirA-ER. The next day, cells were washed 3 times in PBS with 5 mM MgCl_2 (PBS-Mg) and kept thereafter at 4 °C. Cells were incubated for 15 min in PBS-Mg with 1% dialyzed BSA and 0.4 μM Alexa Fluor 555–conjugated traptavidin or streptavidin. For pre-blocking, 50 μM biotin was added to the fluorescent traptavidin 5 min before adding to cells. Cells were washed with PBS/Mg 3 times before imaging live. Cells were imaged using a wide-field DeltaVision Core fluorescent microscope (AppliedPrecision) with a 40 \times oil-immersion lens. ECFP (436DF20 excitation, 480DF40 emission, Chroma 86002v1 dichroic) and Alexa Fluor 555 (540D420 excitation, 600DF50 emission, Chroma 84100bs polychroic) images were collected and analyzed using softWoRx 3.6.2 software. Typical exposure times were 0.1 – 0.5 s and fluorescence images were background-corrected. Different samples in the same experiment were prepared, imaged and analyzed under identical conditions.

AFM analysis. AFM is described in **Supplementary Note 1**.

FtsK displacement assay. For the experiments shown in **Figure 3**, a 439 bp monobiotinylated DNA fragment was generated by PCR with Taq DNA polymerase using primers Fts1 and the internally biotinylated primer bioFts2 (Eurofins) from plasmid pJEG41-P1. This fragment contained two KOPS loading sites (GGGCAGGGGGCAGGG) positioned such that upon addition of ATP, it would take FtsK loaded at KOPS \sim 0.5 s to translocate to streptavidin or traptavidin¹³. *Pseudomonas aeruginosa* FtsK PAK4, a soluble fragment containing the C-terminal 578 residues including the α , β and γ domains and a C-terminal 6His tag, was a kind gift of J. Graham (Oxford University). The protein was overexpressed in *E. coli* and purified by ammonium sulfate precipitation, nickel affinity chromatography and heparin affinity chromatography. The FtsK displacement assay was performed at 25 °C in 20 mM Tris acetate, 2 mM magnesium acetate, 20 mM potassium glutamate and 1 mM dithiothreitol (DTT) (pH 7.5). 16 nM DNA fragment was incubated with 2 μM streptavidin or traptavidin for 10 min, followed by 100 μM biotin to block free biotin binding sites. PAK4 FtsK was added at 0.5 μM in the experiments shown in **Figure 3c,d** and at the indicated concentrations in the experiment shown in **Figure 3e** and allowed to bind to the DNA for 5 min. We added 2 mM ATP to start the reaction and incubated the samples for 3 min for the experiments shown in **Figure 3c,e** and for the indicated times for the experiment shown in **Figure 3d**. Reactions were stopped by adding 1 μl 0.1% SDS with 200 mM EDTA (pH 8.0). Samples were

incubated for a further 15 min to allow FtsK to dissociate from the DNA, mixed with 6× gel loading buffer (1.2 M sucrose, 0.75 mM bromophenol blue; 0.93 mM xylene cyanol FF) and loaded on a 1.5% agarose gel in TAE at 6.0 V cm⁻¹ for 45 min at 25 °C. Ethidium bromide-stained DNA was visualized on a ChemiDoc XRS imager. Percentage free = 100 × intensity of band for free DNA / (intensity of band for free DNA + intensity of band for bound DNA). Percentage displaced = 100 × (% free – % free for negative control) / (100 – percentage free for negative control). Negative values of percentage displaced were rounded up to zero.

For the experiment shown in **Supplementary Figure 4**, a 598-bp monobiotinylated DNA fragment, containing two 8 bp KOPS loading sites 226 bp from the biotinylated end, was generated by PCR with Taq DNA polymerase using primer Fts1 and the terminally biotinylated primer bioFts3 (Sigma-Genosys) (**Supplementary Table 1**) from plasmid pJEG41. *E. coli* FtsK_{50C}, a soluble fragment containing the α, β and γ domains of FtsK, was purified as described³⁰. The FtsK displacement assay was performed at 25 °C in 25 mM Tris (pH 7.5), 10 mM MgCl₂. 5.9 nM DNA fragment was incubated with 0.5 μM streptavidin or traptavidin for 15 min, followed by 100 μM biotin to block free biotin binding sites. 1 μM FtsK_{50C} was added and allowed to bind to the DNA for 5 min. 2.5 mM ATP was added to start the reaction, which was stopped after 2 min with a final concentration of 0.1% SDS and 20 mM EDTA.

Samples were incubated for 20 min and then mixed with 10× gel loading buffer (250 mM Tris (pH 7.5), 20 mM EDTA, 50% glycerol, 2.5% bromophenol blue) before loading on a 1.5% agarose gel in 1× TBE (89 mM Tris, 89 mM boric acid, 2 mM EDTA; pH 8.3) at 10 V cm⁻¹ for 2 h at 25 °C. Gels were stained with SYBR Green (Invitrogen) for 2 h, washed in ddH₂O for 30 min, imaged using a Fuji FLA3000 scanner and quantified using Image Gauge software (Fuji).

17. Beckett, D., Kovaleva, E. & Schatz, P.J. *Protein Sci.* **8**, 921–929 (1999).
18. Howarth, M. *et al. Nat. Methods* **5**, 397–399 (2008).
19. Howarth, M. & Ting, A.Y. *Nat. Protocols* **3**, 534–545 (2008).
20. Sano, T. & Cantor, C.R. *Proc. Natl. Acad. Sci. USA* **87**, 142–146 (1990).
21. Kada, G., Falk, H. & Gruber, H.J. *Biochim. Biophys. Acta* **1427**, 33–43 (1999).
22. Chilkoti, A. & Stayton, P.S. *J. Am. Chem. Soc.* **117**, 10622–10628 (1995).
23. Klumb, L.A., Chu, V. & Stayton, P.S. *Biochemistry* **37**, 7657–7663 (1998).
24. Hyre, D.E. *et al. Protein Sci.* **15**, 459–467 (2006).
25. Green, N.M. *Methods Enzymol.* **184**, 51–67 (1990).
26. Hyre, D.E., Le Trong, I., Freitag, S., Stenkamp, R.E. & Stayton, P.S. *Protein Sci.* **9**, 878–885 (2000).
27. Bayer, E.A., Ehrlich-Rogozinski, S. & Wilchek, M. *Electrophoresis* **17**, 1319–1324 (1996).
28. Qureshi, M.H., Yeung, J.C., Wu, S.C. & Wong, S.L. *J. Biol. Chem.* **276**, 46422–46428 (2001).
29. Qureshi, M.H. & Wong, S.L. *Protein Expr. Purif.* **25**, 409–415 (2002).
30. Lowe, J. *et al. Mol. Cell* **31**, 498–509 (2008).